

## Multi-Gigabit CO-OFDM System over SMF and MMF Links for 5G URLLC Backhaul Network

Amir Haider<sup>1</sup>, MuhibUr Rahman<sup>2</sup>, Tayyaba Khan<sup>3</sup>, Muhammad Tabish Niaz<sup>1</sup> and Hyung Seok Kim<sup>1,\*</sup>

<sup>1</sup>Department of Intelligent Mechatronics Engineering, Sejong University, Seoul, 05006, Korea

<sup>2</sup>Department of Electrical Engineering, Polytechnique Montreal, Montreal, Canada

<sup>3</sup>Department of Telecommunication Engineering, University of Engineering and Technology, Taxila, 47050, Pakistan

\*Corresponding Author: Hyung Seok Kim. Email: hyungkim@sejong.ac.kr

Received: 20 November 2020; Accepted: 15 December 2020

**Abstract:** The 5G cellular network aims at providing three major services: Massive machine-type communication (mMTC), ultra-reliable low-latency communications (URLLC), and enhanced-mobile-broadband (eMBB). Among these services, the URLLC and eMBB require strict end-to-end latency of 1 ms while maintaining 99.999% reliability, and availability of extremely high data rates for the users, respectively. One of the critical challenges in meeting these requirements is to upgrade the existing optical fiber backhaul network interconnecting the base stations with a multigigabit capacity, low latency and very high reliability system. To address this issue, we have numerically analyzed 100 Gbit/s coherent optical orthogonal frequency division multiplexing (CO-OFDM) transmission performance over 400 km single-mode fiber (SMF) and 100 km of multi-mode fiber (MMF) links. The system is simulated over optically repeated and non-repeated SMF and MMF links. Coherent transmission is used, and the system is analyzed in a linear and non-linear regime. The system performance is quantified by bit error ratio (BER). Spectrally efficient and optimal transmission performance is achieved for 400 km SMF and 100 km MMF link. The results designate that MMF links can be employed beyond short reach applications by using them in the existing SMF infrastructure for long haul transmission. In particular, the proposed CO-OFDM system can be efficiently employed in 5G backhaul network. The multi-gigabit capacity and lower BER of the proposed system makes it a suitable candidate especially for the eMBB and URLLC requirements for 5G backhaul network.

**Keywords:** CO-OFDM; coherent transmission; spectrally efficient; optical communication; optical networks; dispersion; eMBB; URLLC; 5G backhaul

### 1 Introduction

The introduction of 5G technology globally is driving radio access network densification, new network architectures, and innovative use cases with stringent performance requirements (e.g., throughput, latency and reliability) [1]. To be successful, network operators need to deploy



This work is licensed under a Creative Commons Attribution 4.0 International License, which permits unrestricted use, distribution, and reproduction in any medium, provided the original work is properly cited.

5G transport technologies that can meet these new requirements in a cost-efficient and timely manner. Traditionally, point-to-point dark fiber has been the transport technology of choice for wireless networks but can quickly become cost prohibitive in certain scenarios [2]. Today, fiber-optic networks play a crucial role in mobile backhaul, supporting over 65% of all macro cell and small cell connections [3]. As 5G deployments continue to accelerate, service providers will need to augment their current fiber networks to stay ahead of growing 5G capacity demands. For operators with their own fiber assets, this may require costly and time-consuming new fiber builds as spare fibers along existing routes are exhausted. One of the key innovations in wireless backhaul is integrated access and backhaul (IAB) [4]. IAB is standardized in 3GPP Release 16 and aims to reuse the existing 5G radio air interface for backhaul purposes as well [5].

As service providers move from initial 5G market launches to building 5G capacity, they are faced with an immediate challenge of securing high bandwidth backhaul solution to the 5G sites in a fast, cost effective manner. mmWave-based 5G deployment increases the challenge of securing optimum backhaul solutions to the sites exponentially. IAB can potentially overcome some of the challenges faced by service providers planning to provide a cost-effective coverage and capacity solution. As a result, there has been significant interest of late in leveraging wavelength division multiplexing (WDM) technology for 5G backhaul [6–8]. A WDM system is also largely transparent to the optical signals it carries. WDM is protocol agnostic and introduces little to no latency, a feature that is particularly important for certain 5G applications and backhaul architectures [9]. Depending on the wavelength grid and the optical transceivers employed, WDM is also capable of supporting individual wavelengths with data rates up to 100 Gbps or more [10]. WDM technology was first developed for and deployed in long-haul fiber-optic networks to maximize system capacity [11]. Using WDM, up to 100 or more wavelengths can be combined (or multiplexed) onto a single fiber, effectively increasing system capacity by 100 times. Over time, as WDM technology has matured it has migrated from long-haul networks to metro networks, and more recently into access and data center networks [12]. The right choice for 5G transport is driven by rigorous technical requirements and the vast array of use cases that 5G technology enables, balanced with real world economic and operational considerations [13].

There has been a lot of advancement in fiber-optics communication systems and networks over the past few years due to the telecommunication sector's ever-increasing requirements. Two streams, which are conspicuous nowadays in optical networks: (a) The rapidly increasing transmission data rate per channel and going beyond 100 Gbit/s, and (b) The use of optical add-drop multiplexers for the dynamically reconfigurable network, are becoming more common. The optical systems face critical challenges due to the fore stated trends in implementing high-speed transmission links [14]. Precisely, for the transmission rate beyond 100 Gbit/s, conventionally preferred optical dispersion compensation and non-linear effects mitigation such as self-phase modulation (SPM), cross-phase modulation (XPM), and four-wave mixing (FWM), are not time and cost-efficient. This is because the dispersion compensation and non-linear effects mitigation require accurate fiber dispersion measurement and precise matching of the dispersion compensation across a broad wavelength range [15].

Recently, the employment of higher-order modulation formats in fiber-optic networking has been observed that heavily rely on digital signal processing (DSP). Several years ago, this similar shift was a prominent feature in the wireless community. Furthermore, the vision of providing high-speed access everywhere to information has led to comprehensive research in advanced modulation formats [16]. Comprising the advantage of scalability to higher-level modulation formats and well-defined spectrum useful for realizing next-generation flexible optical networks [17],

orthogonal frequency division multiplexing (OFDM) has emerged as a promising modulation technique. OFDM is a multi-carrier transmission technique where a data stream is carried with many lower-rate subcarrier tones [18]. In recent years, OFDM has been evolved as a leading physical-layer interface for high-speed wireless communications. Both single carrier and multi-carrier (e.g., OFDM) systems for such DSP-based systems have been proposed [19]. However, OFDM demonstrates distinct advantages over single carriers and is promptly adopted as a dominating modulation format for several wireless community applications [20].

With the increasing interest in coherent receivers, much more effort has been converged on the DSP, which is a key technology for realizing beyond 100 Gbit/s optical transmission system. Coherent optical (CO)-OFDM incorporates the advantages of both ‘coherent detection’ and ‘OFDM modulation.’ It possesses many features that are definite for upcoming high-speed optical fiber transmission systems [21]. Recently, there has been remarkable advancement in CO-OFDM for long-haul transmission [22,23]. CO-OFDM appears to be an appropriate contender for efficient and high capacity transmission by rendering its strength to mitigate the fiber dispersion. Dispersion liveness of CO-OFDM promotes it as an authoritative candidate for multi-mode fiber (MMF)-based transmission. Firstly, the polarization mode dispersion (PMD) and the chromatic dispersion are well predicted and effectively mitigated, while the partially overlapped spectra of OFDM subcarriers ensure high optical spectral efficiency. Secondly, the electrical bandwidth requirement can be reduced for the CO-OFDM transceiver by employing the direct up/down conversion architecture [24]. Thirdly, the innovative algorithm of fast Fourier transform (FFT) or inverse fast Fourier transform (IFFT) can be employed in the OFDM transceiver for the signal processing, which indicates that OFDM can effectively scale the system data rate and overcome the channel dispersion [25].

MMF links are currently drawing much attention for transmission medium of multi-gigabit access networks [26]. Among the in-door installed fibers, multimode silica fiber is at the top of the list. MMF is of enormous demand in LANs due to its prominent features like simplicity in installation, maintenance, and handling, which portray a simple and economical solution [27]. However, inter-modal dispersion limits the capacity of MMF transmission [28]. The center launching technique can minimize the inter-modal dispersion by effectively limiting the MMF’s number of propagating modes [29].

In this paper, the theory and design aspects of CO-OFDM are discussed by reviewing the theoretical fundamentals of CO-OFDM. The proposed design is then simulated to enhance transmission capacity for optical networks by employing CO-OFDM for MMF links for long haul transmissions. In particular, the employment of such a system to meet the requirement of eMBB and URLLC services of 5G networks is demonstrated.

## 2 Theoretical Principle of Coherent Optical OFDM

In general, an optical OFDM system consists of five major functional blocks, which are: Radio frequency (RF) OFDM transmitter, RF-to-optical (RTO) up-converter, an optical link, an optical-to-RF (OTR) down-converter, and RF OFDM receiver [30]. Fig. 1 shows the generic block diagram of the CO-OFDM system.

Due to OFDM’s drastic liveness to the channel dispersion in the optical domain, it has been widely investigated for many applications [31]. The key proposition of OFDM is its linear modulation and demodulation while keeping linearity in propagation too. Furthermore, a linear transformation is a key goal for the OFDM implementation. So, the main challenge faced for

CO-OFDM implementation is the realization of a linear RTO up-converter as well as a linear OTR down-converter. To address this challenge, a linear conversion between the RF signal and optical field signal is achieved by biasing the Mach-Zehnder modulators (MZM) at the null point [32]. With coherent detection, linearity in transformation can be ensured while going from optical field signal to RF (or electrical) signal [33]. Keeping in view the aspects mentioned above, it is feasible to model a linear channel that ensures OFDM's best performance by canceling the impact of channel dispersion in both the RF domain and optical domain [34].

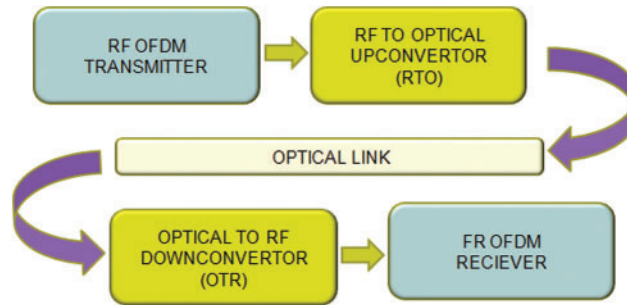


**Figure 1:** Block diagram of a generic CO-OFDM system

### 3 Simulation Model and Optimization Scheme

In this paper, a CO-OFDM system is simulated using direct up/down conversion architecture for data rate 100 Gbit/s over SMF and MMF links. Fig. 2 shows the simulation model of the proposed scheme. A dual-polarization RF transmitter capable of generating two RF OFDM signals is designed to support the transmission data rate of 100 Gbit/s. For each polarization, the RF OFDM transmitter uses 128 points FFT, out of which only the middle 82 subcarriers are effectively used as data. The guard interval is 1/8th of the observation window, and four of them are used for phase estimation. The modulation format is 4-QAM on each subcarrier. For each polarization of the RF OFDM transmitter, two  $2^{13-1}$  PBRs generators are used as a data source. To convert the RF signals to optical domain, RTO up-convertors are employed. Each RTO up-converter contains two MZMs. One modulator is for the real part of the input signal, while the other with  $90^\circ$  phase shift is for the imaginary part of the input signal. A continuous-wave (CW) laser is used as the optical modulator at a wavelength of 1550 nm. Four spans of SMF, each having length of 100 km, are used to design the optical link for transmission up to 400 km. For the SMF, the attenuation coefficient  $\alpha$ , dispersion coefficient  $\beta$ , and non-linear coefficient  $\gamma$  are taken to be 0.2 dB/km, 16 ps/nm · km, and  $1.2 \text{ w}^{-1} \cdot \text{km}^{-1}$ , respectively. An erbium-doped fiber amplifier (EDFA) with a gain of 20 dB/span and noise figure of 4.5 dB is used as an optical amplifier to compensate for the transmission losses, while dispersion-compensating fiber (DCF) is used to compensate for dispersion. For the DCF, the attenuation coefficient  $\alpha$ , dispersion coefficient  $\beta$ , and non-linear coefficient  $\gamma$  are taken to be 0.5 dB/km,  $-80 \text{ ps/nm} \cdot \text{km}$ , and  $4.5 \text{ w}^{-1} \cdot \text{km}^{-1}$ , respectively. In the next investigation, a single span of 20 km MMF is used, followed by 5 spans of 20 km MMF to achieve a transmission distance of 100 km. The signal launch power is varied at the transmitter, and it is propagated through the MMF's fundamental mode. At the receiver end, a dual-polarization optical receiver is used, which converts the optical signal to electrical using OTR down-converters; each of them comprises four photoelectric PIN

diodes and is observed through an eye-diagram analyzer. To model the local oscillator (LO), a CW laser is used. Bit error rate (BER) and Q-factor are used to quantify the system performance.

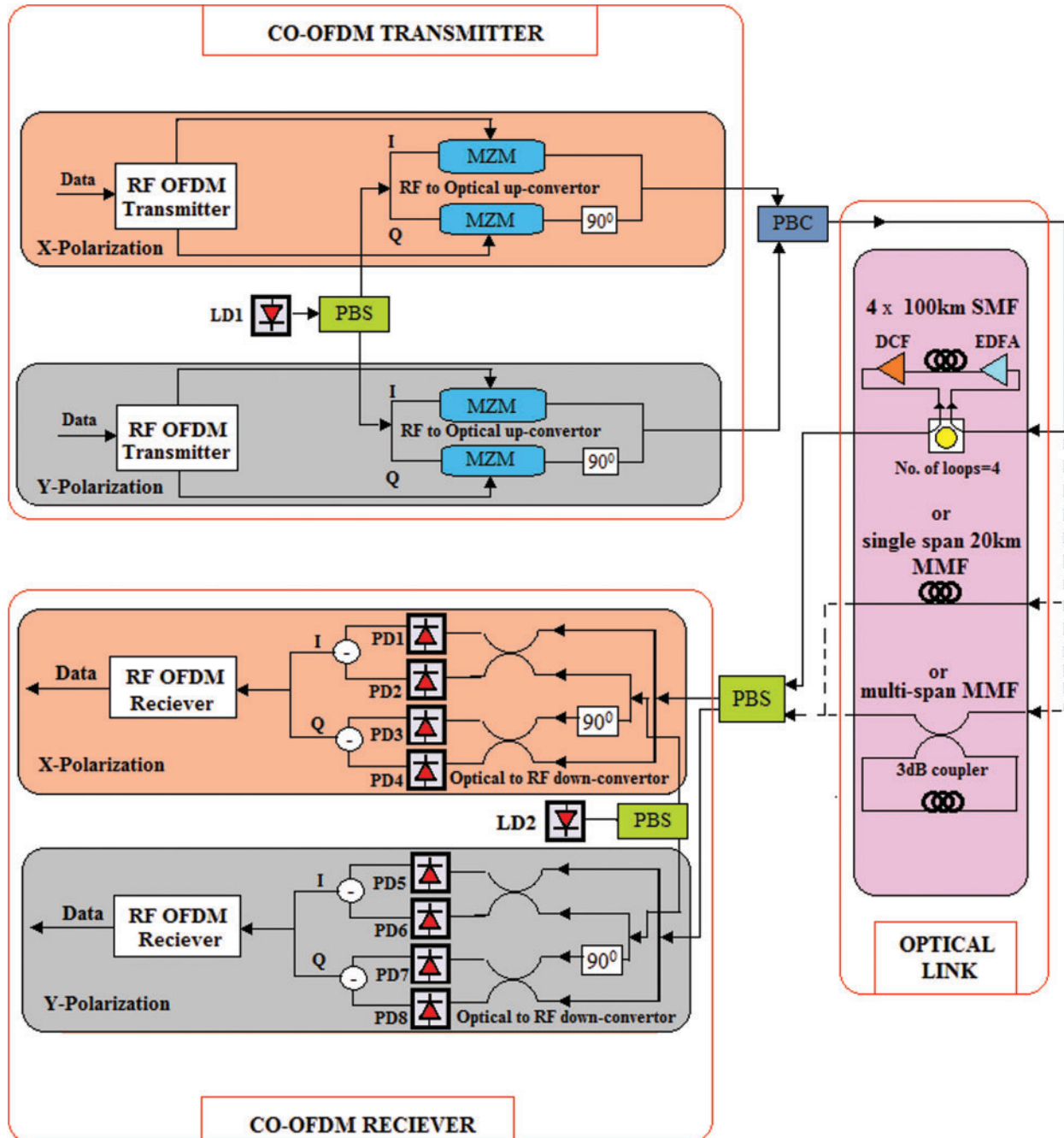
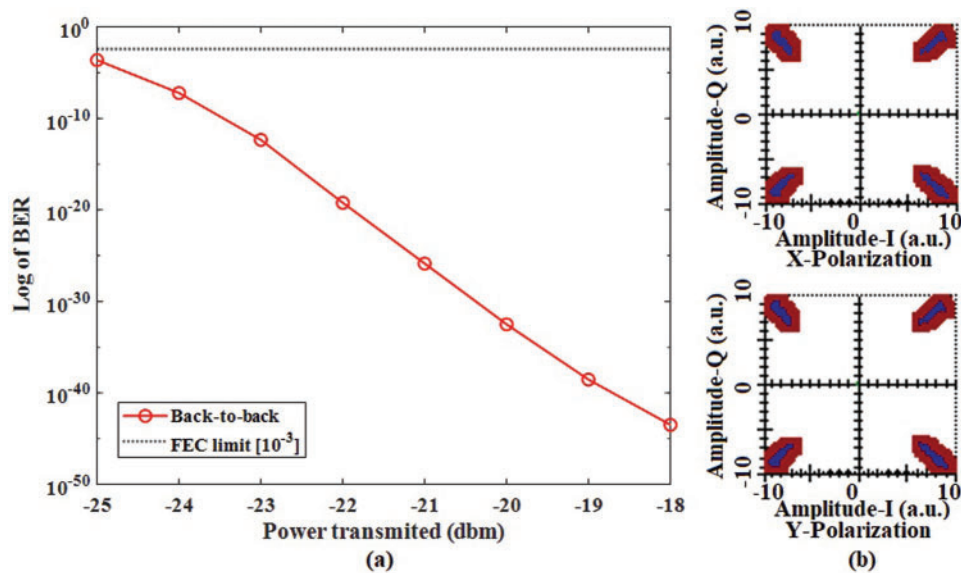


Figure 2: Proposed model of CO-OFDM system

The simulation parameters used are summarized in [Tab. 1](#).

**Table 1:** Parameters used for simulation at 1550 nm

Simulation parameters	Values
Data rate	100 Gbit/s
No. of FFT points	128
Modulation format	4-QAM
Total transmission distance for SMF	400 km
Total transmission distance for MMF	100 km
Attenuation coefficient of SMF	0.2 dB/km
Attenuation coefficient of MMF	0.7 dB/km
Core diameter of SMF	10 $\mu\text{m}$
Core diameter of MMF	50 $\mu\text{m}$



**Figure 3:** (a) BER as a function of launched power into the transmitter for back to back transmission (b) X- and Y-polarization constellation diagrams

## 4 Simulation Results and Discussion

### 4.1 Back-to-Back Transmission

Back-to-back transmission with a non-amplified optical link is first simulated for the proposed system. While the transmission characteristics of SMF/MMF fiber transmission are monitored, the effect of PMD and laser linewidth is ignored in our first analysis. The BER against the transmitter's launched power is shown in [Fig. 3a](#) for back-to-back transmission. The vertical axis represents the log of BER, while the horizontal axis represents the launched power. It is observed that the BER improves with an increase in transmitted power, which in turn tends to improve the Q-factor. The transmission maintains the forward error correction (FEC) limit of  $10^{-3}$  for the

whole range of launched power from  $-25$  dBm to  $-18$  dBm. The received X- and Y-polarization constellation diagrams of the CO-OFDM signal for the 4-QAM modulation scheme are shown in Fig. 3b, which ensures optimal transmission with minimum BER for back-to-back transmission.

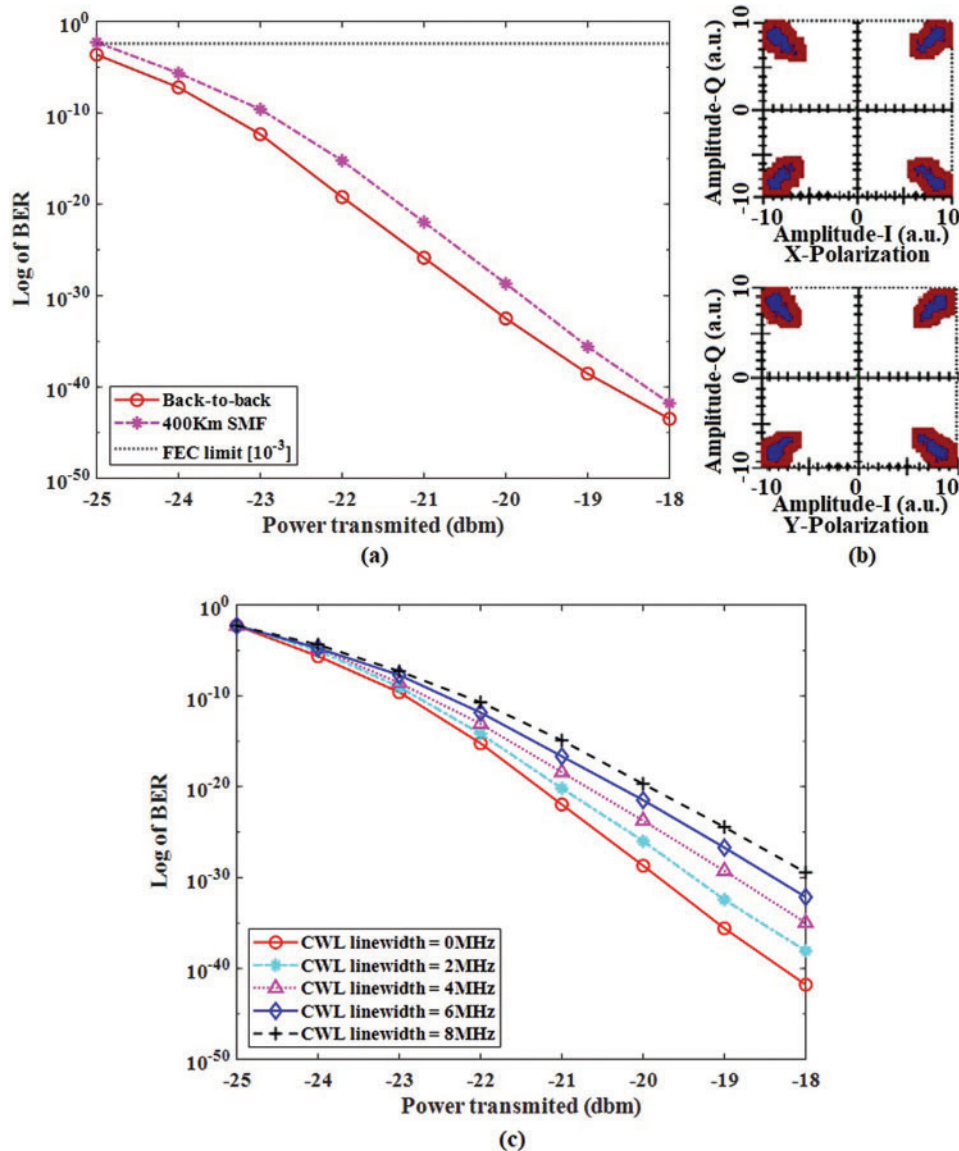


**Figure 4:** (a) BER as a function of launched power into the transmitter for 400 km SMF transmission (b) X- and Y-polarization constellation diagrams (c) variation in BER vs. the launched power with CW laser linewidth variation

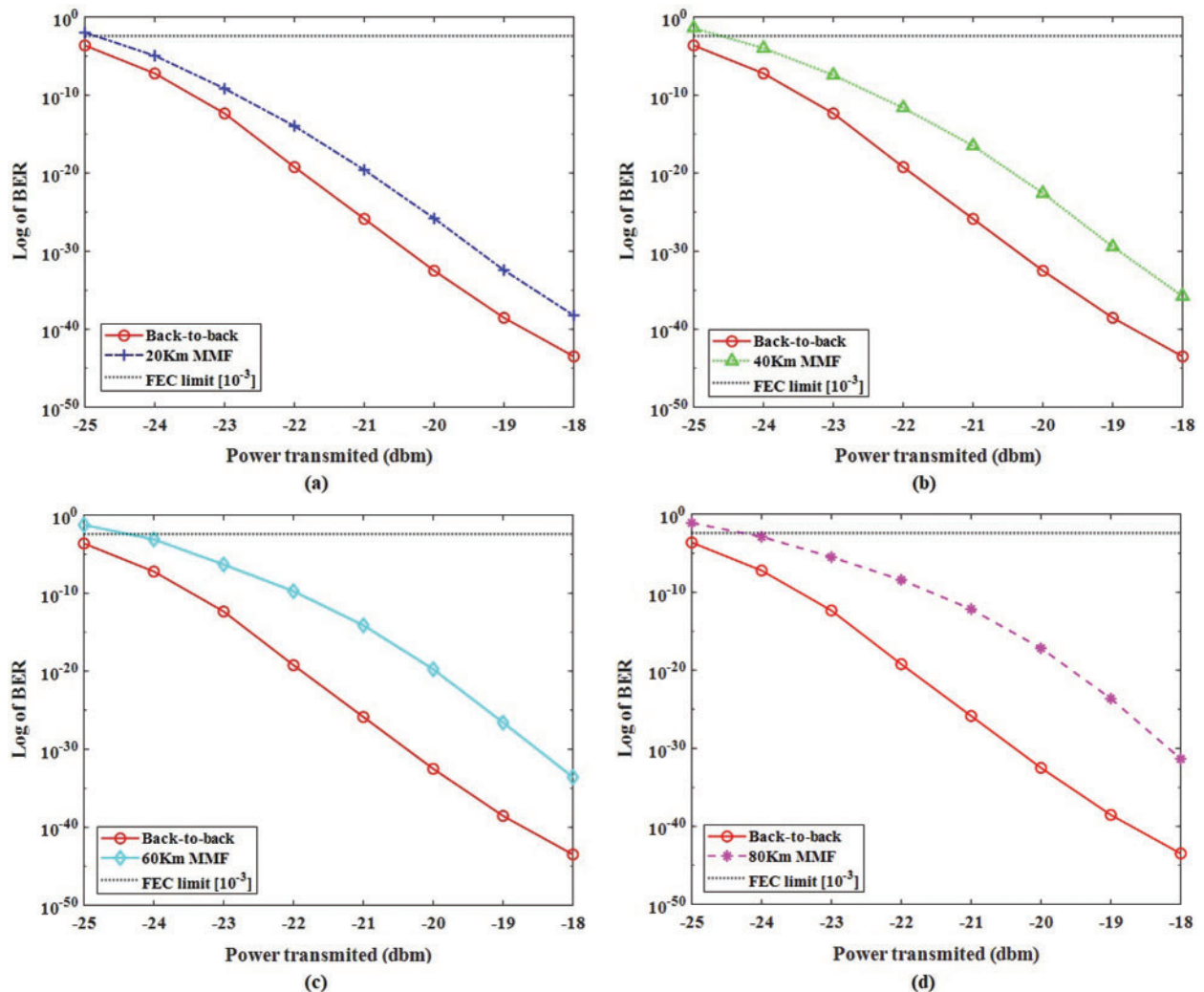


**Figure 5:** BER as a function of launched power into the transmitter for (a) 20 km MMF link (b) 40 km MMF link (c) 60 km MMF link (d) 80 km MMF link

#### 4.2 400 km Single-Mode Fiber Link

Amplified SMF link transmission is then simulated with the proposed system. The optical link contains 4 spans of SMF, each of length 100 km for transmission up to 400 km. For the SMF, the attenuation coefficient  $\alpha$ , dispersion coefficient  $\beta$ , and non-linear coefficient  $\gamma$  are taken to be 0.2 dB/km, 16 ps/nm.km, and  $1.2 \text{ w}^{-1} \cdot \text{km}^{-1}$ , respectively. An EDFA with a gain of 20 dB/span and noise figure of 4.5 dB is used as an optical amplifier to compensate for the transmission losses, while DCF is used to compensate for dispersion. For the DCF, the attenuation coefficient  $\alpha$ , dispersion coefficient  $\beta$ , and non-linear coefficient  $\gamma$  are taken to be 0.5 dB/km,  $-80 \text{ ps/nm} \cdot \text{km}$ , and  $4.5 \text{ w}^{-1} \cdot \text{km}^{-1}$ , respectively. Simulation is done for linewidth of modulating CW laser at 0, 2, 4, 6, and 8 MHz. The results of BER against launched power into the transmitter are shown in Fig. 4a for 400 km SMF transmission. The vertical axis represents the log of BER, while the horizontal axis represents the launched power. It is observed that the BER



improves with an increase in transmitted power, which in turn tends to improve the Q-factor. The FEC limit is maintained in the transmission for launched power from  $-25$  to  $-18$  dBm. The received X- and Y-polarization constellation diagrams of the CO-OFDM signal for the 4-QAM modulation scheme are shown in Fig. 4b, which ensures optimal transmission with minimum BER for SMF transmission link. Fig. 4c shows the variation in BER vs. launched power graph with the change in CW laser linewidth. It is observed that increasing the laser linewidth degrades the Q-factor. This results in a decrease in BER, so the system is less immune to dispersion. In this work, the CW laser linewidth is taken to be 0 MHz.

### 4.3 20–100 km Multi-Mode Fiber Link

MMF link transmission is then simulated with the proposed system. MMF optical link contains 5 spans of MMF, each of length 20 km for transmission up to 100 km. Simulation is done for the attenuation coefficient of MMF at 0.7 dB/km. The results of BER against launched power into the transmitter are shown in Fig. 5a–5d for 20, 40, 60, 80 km MMF transmission links, respectively. The vertical axis represents the log of BER, while the horizontal axis represents the launched power. It is observed that the BER improves with an increase in transmitted power, which in turn tends to improve the Q-factor. Inter-modal dispersion is minimum in 20 km MMF link and increases as we increase the transmission distance.

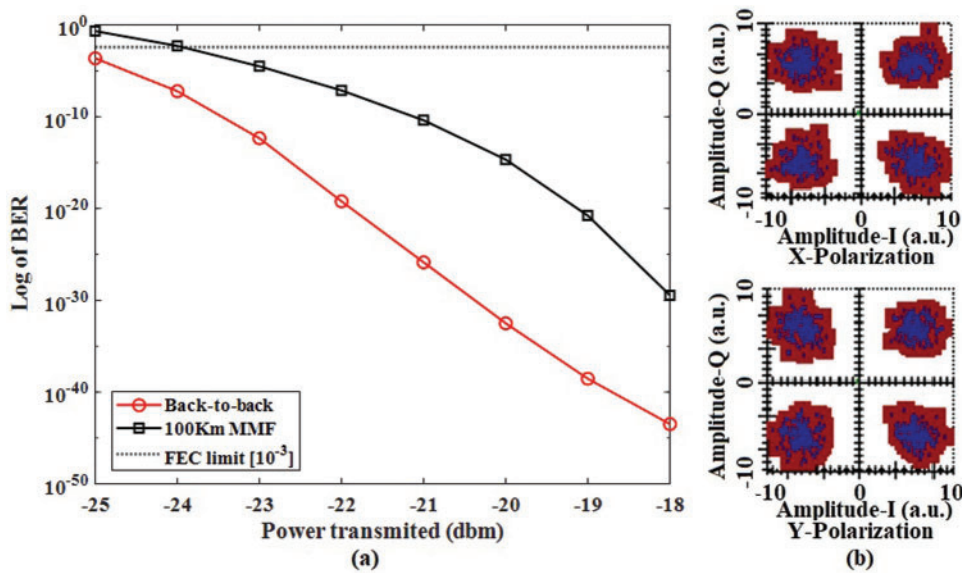


**Figure 6:** (a) BER as a function of launched power into the transmitter for 100 km SMF transmission (b) X- and Y-polarization constellation diagrams

The results for 100 km MMF link transmission are shown in Fig. 6. Fig. 6a shows the results of the bit error rate (BER) against launched power into the transmitter for 100 km MMF transmission link. The vertical axis represents the log of BER, while the horizontal axis represents the launched power. It is observed that the BER improves with an increase in transmitted power, which in turn tends to improve the Q-factor. The FEC limit is maintained in the transmission for launched power from  $-24$  to  $-18$  dBm. The 4-QAM modulation scheme received X- and Y-polarization constellation diagrams of the CO-OFDM signal are shown in Fig. 6b, which

ensures optimal transmission with minimum BER for 100 km MMF transmission link. Fig. 7 summarizes the variation in BER vs. launched power for 20, 40, 60, 80, and 100 km MMF transmission links. With variation in the transmitter's power levels and increased transmission distance, degradation in Q-factor and resulting BER are observed, increasing dispersion. Inter-modal dispersion is minimum in 20 km MMF link and increases as we increase the transmission distance. In the 100 km MMF link, the dispersion level is higher.

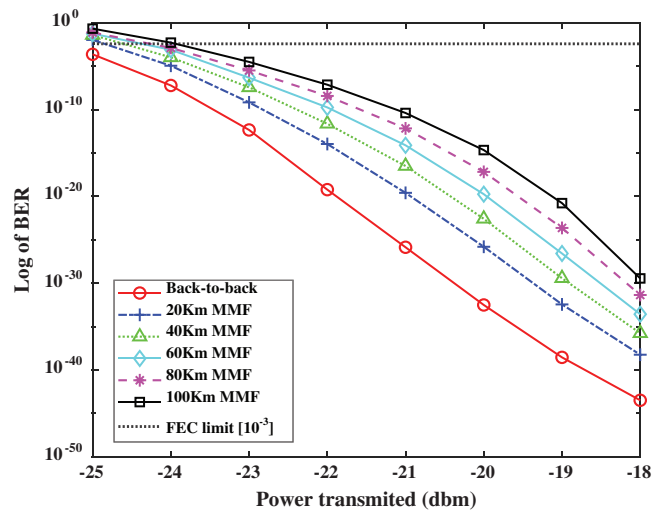


**Figure 7:** Summary of BER vs. launched power variation for 20, 40, 60, 80, and 100 km MMF transmission links

## 5 Conclusions

We have numerically analyzed the performance of 100 Gbit/s CO-OFDM transmission over 400 km SMF and 100 km MMF fiber links. The system is simulated over optically repeated and non-repeated SMF and MMF links. Coherent transmission is used, and the system is analyzed in linear and non-linear regimes. The system performance is quantified by BER. Both X- and Y-polarizations show similar results. The maximum Q-factor is stabilized for a wide range from  $-24$  to  $4$  dBm launch power into MMF. With variation in the transmitter's power levels, and an increase in transmission distance, degradation in Q-factor and resulting BER is observed, which show an increase in inter-modal dispersion. This effect is minimum in 20 km MMF link and increases as we increase the transmission distance. The SMF and MMF links results are closely correlated, which show that MMF can be used as transmission link in existing infrastructure of SMF provided the mitigation of intermodal dispersion and non-linear effects by using modulation format like CO-OFDM. The results signify that the MMF link can be employed beyond short-reach applications by using them in the existing SMF infrastructure for long haul transmission. In particular, the proposed system can be efficiently employed in 5G backhaul network. The multi-gigabit capacity and lower BER of the proposed system makes it a suitable candidate especially for the eMBB and URLLC requirements for 5G backhaul network.

**Funding Statement:** This work was supported by the National Research Foundation of Korea (NRF) grant funded by the Korean government (MSIT) (Nos. 2019R1A4A1023746, 2019R1F1A1060799) and the Strengthening R&D Capability Program of Sejong University.

**Conflicts of Interest:** The authors declare that they have no interest in reporting regarding the present study.

## References

- [1] S. Henry, A. Alsohaily and E. S. Sousa, “5G is real: Evaluating the compliance of the 3GPP 5G new radio system with the ITU IMT-2020 requirements,” *IEEE Access*, vol. 8, no. 1, pp. 42828–42840, 2020.
- [2] J. J. Pedreno-Manresa, P. S. Khodashenas, M. S. Siddiqui and P. Pavon-Marino, “On the need of joint bandwidth and NFV resource orchestration: A realistic 5G access network use case,” *IEEE Communications Letters*, vol. 22, no. 1, pp. 145–148, 2017.
- [3] A. Douik, H. Dahrouj, T. Y. Al-Naffouri and M. S. Alouini, “Hybrid radio/free-space optical design for next generation backhaul systems,” *IEEE Transactions on Communications*, vol. 64, no. 6, pp. 2563–2577, 2016.
- [4] C. Saha and H. S. Dhillon, “Millimeter wave integrated access and backhaul in 5G: Performance analysis and design insights,” *IEEE Journal on Selected Areas in Communications*, vol. 37, no. 2, pp. 2669–2684, 2019.
- [5] 3GPP RP-193251, “Enhancements of Integrated Access and Backhaul (Release 16/17),” in *3GPP TSG RAN Meeting Proc.*, 2019. [Online]. Available: [https://www.3gpp.org/ftp/tsg\\_ran/TSG\\_RAN/TSGR\\_86/Docs](https://www.3gpp.org/ftp/tsg_ran/TSG_RAN/TSGR_86/Docs).
- [6] J. Zou, C. Wagner and M. Eiselt, “Optical fronthauling for 5G mobile: A perspective of passive metro WDM technology,” in *Proc. OFC*, Los Angeles, CA, USA, pp. 1–3, 2017.
- [7] Commscope, “How WDM helps with 5G deployment,” 2017. [Online]. Available: <https://www.commscope.com/blog/2017/how-wdm-helps-with-5g-deployment/>.
- [8] CableLabs, “P2PCO-SP-ARCH-I02-190311-P2P coherent optics architecture specification,” Louisville, CO: CableLabs, 2019. [Online]. Available: <https://www.cablelabs.com/specifications/P2PCO-SP-ARCH>.
- [9] D. Zhang, D. Zhe, M. Jiang and J. Zhang, “High speed WDM-PON technology for 5G fronthaul network,” in *Proc. ACP*, Hangzhou, China, pp. 1–3, 2018.
- [10] F. Musumeci, G. Belgiovine and M. Tornatore, “Dynamic placement of baseband processing in 5G WDM-based aggregation networks,” in *Proc. OFC*, Los Angeles, CA, USA, pp. 1–3, 2017.
- [11] T. R. Raddo, S. Rommel, B. Cimoli and I. T. Monroy, “The optical fiber and mmwave wireless convergence for 5G fronthaul networks,” in *Proc. 5GWF*, Dresden, Germany, pp. 607–612, 2019.
- [12] K. Igarashi, T. Tsuritani, I. Morita and M. Suzuki, “Ultra-long-haul high-capacity super-Nyquist-WDM transmission experiment using multi-core fibers,” *Journal of Lightwave Technology*, vol. 33, no. 5, pp. 1027–1036, 2015.
- [13] Q. Wang, J. Alcaraz-Calero, R. Ricart-Sanchez, M. B. Weiss, A. Gavras *et al.*, “Enable advanced QoS-aware network slicing in 5G networks for slice-based media use cases,” *IEEE Transactions on Broadcasting*, vol. 65, no. 2, pp. 444–453, 2019.
- [14] H. Kashif, M. N. Khan and A. Altalbe, “Hybrid optical-radio transmission system link quality: Link budget analysis,” *IEEE Access*, vol. 8, no. 1, pp. 65983–65992, 2020.
- [15] F. Gholami, E. Myslivets, S. Zlatanovic, N. Alic and S. Radic, “Dispersion characterization of highly nonlinear fiber over a 700-nm band,” *IEEE Photonics Technology Letters*, vol. 24, no. 12, pp. 1021–1023, 2012.
- [16] N. Cvijetic, A. Tanaka, M. Cvijetic, Y. K. Huang, E. Ip *et al.*, “Novel optical access and digital processing architectures for future mobile backhaul,” *Journal of Lightwave Technology*, vol. 31, no. 4, pp. 621–627, 2013.

- [17] J. Pedro, "Designing transparent flexible-grid optical networks for maximum spectral efficiency," *IEEE/OSA Journal of Optical Communications and Networking*, vol. 9, no. 4, pp. 35–44, 2017.
- [18] C. Jing, X. Tang, X. Zhang, L. Xi and W. Zhang, "Time domain synchronous OFDM system for optical fiber communications," *China Communications*, vol. 16, no. 9, pp. 155–164, 2019.
- [19] K. Mizutani, T. Matsumura and H. Harada, "A comprehensive study of universal time-domain windowed OFDM-based LTE downlink system," in *Proc. WPMC*, Bali, Indonesia, pp. 28–34, 2017.
- [20] F. D. Stasio, M. Mondin and F. Daneshgaran, "Multirate 5G downlink performance comparison for f-OFDM and w-OFDM schemes with different numerologies," in *Proc. ISNCC*, Rome, Italy, pp. 1–6, 2018.
- [21] G. Bosco, A. Carena, V. Curri, P. Poggiolini and F. Forghieri, "Performance limits of nyquist-WDM and CO-OFDM in high-speed PM-QPSK systems," *IEEE Photonics Technology Letters*, vol. 22, no. 15, pp. 1129–1131, 2010.
- [22] G. Shen, S. You, Q. Yang, Z. He, N. Yang *et al.*, "Experimental demonstration of CO-OFDM optical network with heterogeneous ROADMs nodes and variable channel bit-rates," *IEEE Communications Letters*, vol. 15, no. 8, pp. 890–892, 2011.
- [23] L. Xu, J. Chen, Z. Feng, Q. Wu, M. Tang *et al.*, "Long haul quasi-single-mode transmission using raman amplified hybrid FMF/SSMF span for CO-OFDM system," in *Proc. OECC-PGC*, Singapore, pp. 1–3, 2017.
- [24] X. Du, T. Song and P. Y. Kam, "Carrier frequency offset estimation for CO-OFDM: The matched-filter approach," *Journal of Lightwave Technology*, vol. 36, no. 14, pp. 2955–2965, 2018.
- [25] S. Mhatli, H. Mrabet and A. Amari, "Extensive simulation of fiber non-linearity mitigation in a CO-OFDM-WDM long-haul communication system," *IET Optoelectronics*, vol. 12, no. 5, pp. 258–262, 2018.
- [26] J. M. Castro, R. Pimpinella, B. Kose, P. Huang, B. Lane *et al.*, "Investigation of 60 Gb/s 4-PAM using an 850 nm VCSEL and multimode fiber," *Journal of Lightwave Technology*, vol. 34, no. 16, pp. 3825–3836, 2016.
- [27] J. James, P. Shen, A. Nkansah, X. Liang and N. J. Gomes, "Millimeter-wave wireless local area network over multimode fiber system demonstration," *IEEE Photonics Technology Letters*, vol. 22, no. 9, pp. 601–603, 2010.
- [28] Y. Zhao, S. Huang, C. Yan and X. Shen, "Mode dispersion analysis based on refractive index of graded-index multimode fiber," in *Proc. ACP*, Hangzhou, China, pp. 1–3, 2018.
- [29] T. Cseh and T. Berceci, "Efficient compensation methods for modal dispersion in radio over multimode fiber links," in *Proc. MIKON*, Gdansk, Poland, pp. 1–3, 2014.
- [30] S. Hussin, K. Puntsri and R. Noé, "Performance analysis of optical OFDM systems," in *Proc. ICUMT*, Budapest, Hungary, pp. 1–5, 2011.
- [31] J. Zhao and A. Ellis, "Advantage of optical fast OFDM over OFDM in residual frequency offset compensation," *IEEE Photonics Technology Letters*, vol. 24, no. 24, pp. 2284–2287, 2012.
- [32] G. Magazzù, G. Ciarpì and S. Saponara, "Design of a radiation-tolerant high-speed driver for mach-zehnder modulators in high energy physics," in *Proc. ISCAS*, Florence, Italy, pp. 1–5, 2018.
- [33] S. Adhikari, S. L. Jansen, M. Alfiad, B. Inan, V. A. J. M. Sleiffer *et al.*, "Self-coherent optical OFDM: An interesting alternative to direct or coherent detection," in *Proc. ICTON*, Stockholm, Sweden, pp. 1–4, 2011.
- [34] K. A. Al-Khateeb, F. Akhter and M. R. Islam, "Impact of fiber optic dispersion on the performance of OFDM-QAM system," in *ICCCE'10*, Kuala Lumpur, Malaysia, pp. 1–5, 2010.